Multispectral and low-filling-factor superconducting nanowire single photon detector with high absorption efficiency

Dezhi Li, Xiangyuan Liu and Rongzhen Jiao

COLLECTIONS

Paper published as part of the special topic on Photonics and Optics

View Online   Export Citation   CrossMark

ARTICLES YOU MAY BE INTERESTED IN
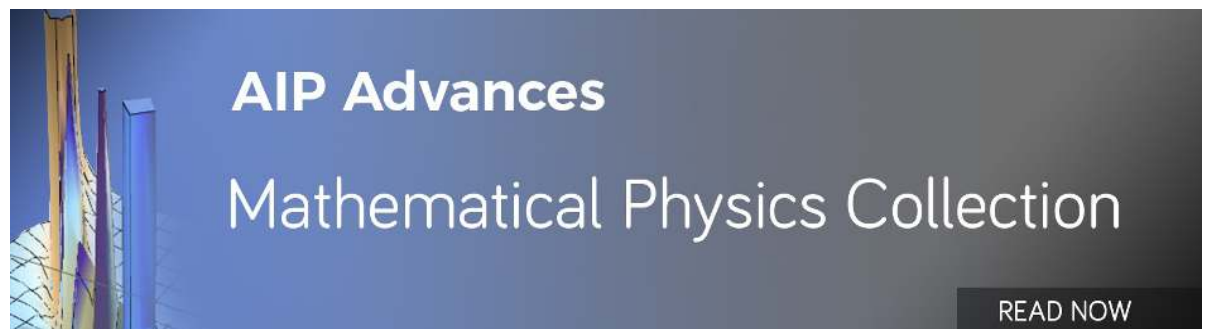
AIP Advances

Mathematical Physics Collection

READ NOW

Multispectral and low-filling-factor superconducting nanowire single photon detector with high absorption efficiency

View Online   Export Citation   CrossMark

Dezhi Li,[1,2] (iD) Xiangyuan Liu,[1,2] and Rongzhen Jiao[1,2,a)] (iD)

AFFILIATIONS

[1] State Key Laboratory of Information Photonics and Optical Communications, Beijing University of Posts
  and Telecommunications, Beijing 100876, China
[2] School of Science, Beijing University of Posts and Telecommunications, Beijing 100876, China

[a)] Author to whom correspondence should be addressed: rzjiao@bupt.edu.cn

ABSTRACT

We propose a superconducting nanowire single photon detector (SNSPD) that can work efficiently at two target wavelengths and has a significant improvement in the counting rate due to the low-filling-factor nanowires in the silicon slots and the silver reflector. Numerical simulations show that the absorption efficiency can be over 90% at a single wavelength, whether the incident light wavelength is 1550 nm or 1064 nm, and over 80% when the SNSPD is designed to work at both wavelengths. In addition, the reset time is about 24% of the conventional SNSPDs. Our work presents a design for fabricating faster, larger-area, and multispectral SNSPDs with a high efficiency, which can be applied in applications such as quantum optics communication and multiwavelength sensing.

I. INTRODUCTION

In the past decade, superconducting nanowire single photon detectors (SNSPDs)[1] have attracted dynamic attention owing to their excellent performances, such as high system detection efficiency (SDE),[2] low dark count rate (DCR),[3] high count rate,[4,5] and low time jitter,[6] thereby enabling numerous applications, including measurement-device-independent quantum key distribution,[7] quantum random number generator,[8] ultra-long range optical communication,[9] and single photon quantum imager.[10] These applications make full use of the accurate and fast response characteristics of the SNSPDs; therefore, the performances of SNSPDs are vital to the development of other optical fields.

Optical absorption efficiency is an important contribution to the SDE. To improve the absorption efficiency, which is determined by the structure of the SNSPDs and the material of the superconducting nanowires,[11] various methods were proposed, such as SNSPDs with the optical cavity and anti-reflection coating,[12] SNSPDs with optical nano-antennas,[13] waveguide integrated SNSPDs,[14] and using amorphous WSi as the superconducting

material.[2,15] These methods generally confined the incident photons in the optical cavities, and decreased the reflection and transmission of SNSPDs, thus improving the absorption efficiency of the nanowires. Furthermore, the superconducting materials with better properties were applied. However, these designed devices suffered from two problems. One is that most of the reported SNSPDs showed a high SDE only at a single resonant wavelength due to the resonant effect of the optical cavity,[12] though superconducting nanowires are intrinsically wideband. With the extension of the use of SNSPDs from near infrared to visible light, many studies were focused on designing and fabricating broadband[16] or multispectral[17] SNSPDs to meet the practical requirements. The other is that trade-off between the optical absorption efficiency and the counting rate, a parameter characterizing the detection speed of the SNSPDs.[18] The counting rate is limited by the recovery time of the bias current, which is determined by the kinetic inductance of nanowires,[19,20] and the kinetic inductance is proportional to the length of nanowires. However, most of these devices have long and dense meander nanowires to absorb photons; hence, the counting rate of these devices is usually limited. Thus, in order to

satisfy the complex requirements, it is important to consider how to manufacture the SNSPDs to meet the conditions of high SDE, high counting rate, and multiple detection wavelengths simultaneously.

In this paper, we present a strategy to solve the two problems that are referred to above by using the nanowires in the silicon slots and the silver reflector. The electric field near the nanowires is strongly enhanced whether the wavelength of the incident light is 1550 nm or 1064 nm. Meanwhile, a high optical absorption efficiency can be achieved even for the low-filling-factor nanowires. It is an improvement to the conventional SNSPDs, which generally work with 50% filling factor and a single wavelength. Here, the filling factor is defined as the nanowire width divided by the pitch of the nanowire. We report on a multispectral and low-filling-factor SNSPD with a high optical absorption efficiency and a high counting rate and analyze its performances systematically.

II. OPTICAL ABSORPTION EFFICIENCY

In practice, the nanowires in a conventional SNSPD is normally fabricated in a meander pattern, which can be simplified as a two-dimension periodic structure. The optical absorption efficiency (denoted by A) of superconducting nanowires is calculated as[21]

$$A = \frac{\int_{-w/2}^{w/2} \int_0^t w \mathrm{Im}[\varepsilon]|E|^2 dx dy}{\int_{-p/2}^{p/2} (\frac{\varepsilon_0}{\mu_0})^{1/2} |E_0|^2 dx}, \qquad (1)$$

where w and t are the width and thickness of the nanowires, respectively; p is the pitch of the period unit; E_0 is the electric field intensity of the incident light; E is the electric field intensity within the nanowires; ε is the dielectric constant of the nanowires; and ε_0 and μ_0 denote the permittivity and permeability of the background material, respectively.

The designed structure includes the silver (Ag) reflector, silicon (Si) and hydrogen silsesquioxane (HSQ) slots, NbN nanowires, and the sapphire substrate from top to bottom, as illustrated in Fig. 1. The stack structure with the optical microcavity was widely applied in the design and manufacture of the SNSPDs.[13,22] To investigate the relationship between the structure parameters and the optical absorption efficiency, a commercial numerical simulation software,

i.e., FDTD Solutions (by Lumerical, Inc.) was applied. The thicknesses of Ag, Si, and HSQ layers are 130 nm, 400 nm, and 400 nm, respectively. In addition, the width of NbN nanowires (W) was fixed to 80 nm, a typical parameter of the nanowires in SNSPDs. In the following simulations, complex refractive indices $n_{sapphire} = 1.74$, $n_{HSQ} = 1.4$, $n_{NbN} = 4.905 + i4.293$, $n_{Si} = 3.628$, and $n_{Ag} = 0.322 + i10.99$ were used.[18] The region surrounded by the dashed line is the period unit for electromagnetic simulations. The incident light used in the simulations is incident from the bottom and is transverse magnetic (TM) polarized. Periodic boundary conditions were used in the numerical simulations, and the edge effect of the meander nanowires were neglected.

Two typical near-infrared wavelengths (1064 nm and 1550 nm) were selected in the following electromagnetic simulations. The thickness of the NbN nanowires is 4 nm. To demonstrate the superior performance of the proposed SNSPD, it was compared with the conventional SNSPDs with Ag slots in the following discussion.[13] The calculated absorption efficiency dependence of the pitch are shown in Fig. 2(a). Due to the Si–HSQ–Si slots, the optical absorption efficiency of the nanowires can be over 90% whether the wavelength of the incident light is 1550 nm or 1064 nm, though the pitch is as large as 732 nm or 674 nm. The corresponding filling-factor is about 10.9% or 11.9%. In addition, the absorption efficiencies of

(a)

(b)
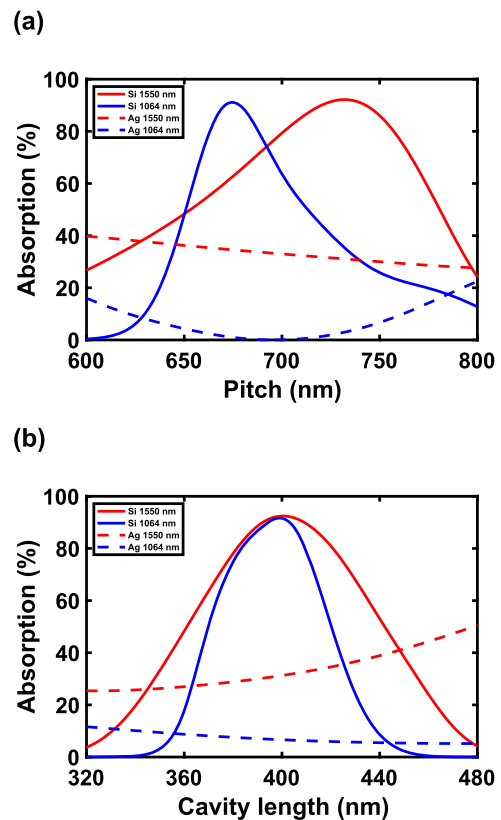
FIG. 2. Simulated pitch (a) and cavity length (b) dependence of the optical absorption efficiency in the nanowire. Solid and dashed lines represent the proposed SNSPD with Si slots and conventional SNSPDs with Ag slots, respectively.
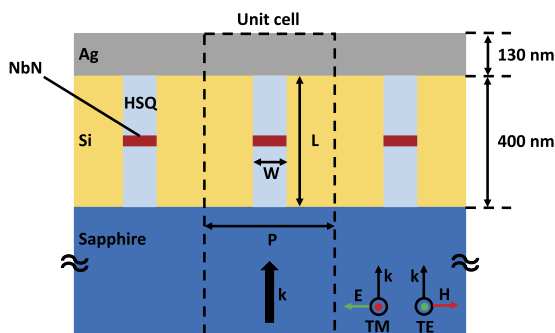

FIG. 1. Schematic of the stack structure of the proposed SNSPD. The pitch of the period unit, the length of the cavity, and the width of the nanowires are denoted by P, L, and W, respectively. The direction of the incident light is marked by the black arrow and the incident light is TM-polarized.

FIG. 3. Electric field intensity distribution in the period unit. (a) The incident light wavelength is 1550 nm and the pitch is 732 nm. (b) The incident light wavelength is 1064 nm and the pitch is 674 nm.
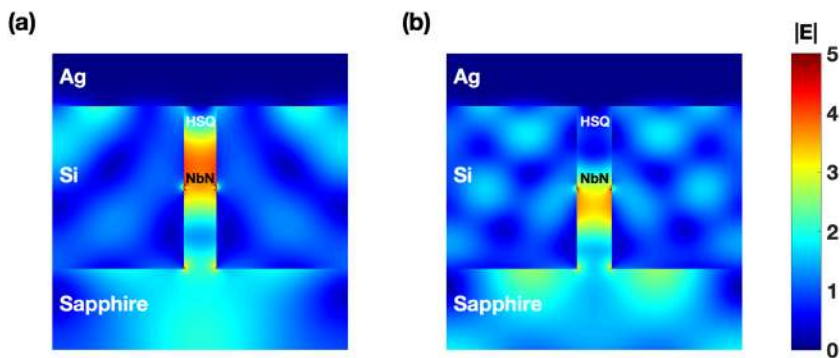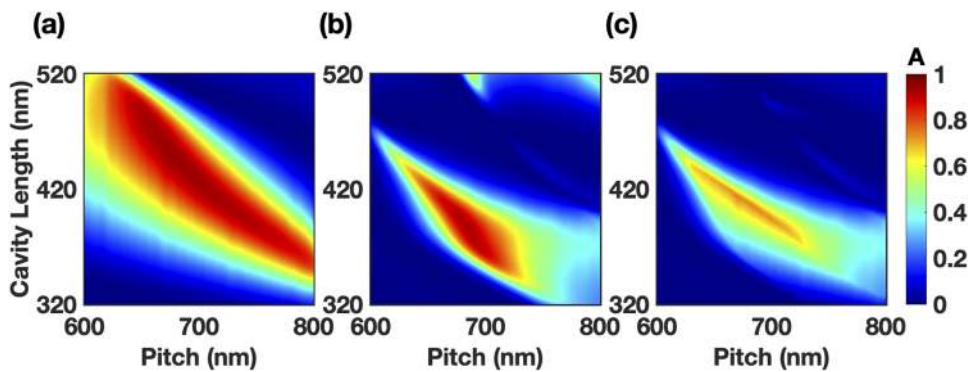

FIG. 4. Simulated structure parameters dependence of the optical absorption efficiency. The incident light wavelengths are 1550 nm (a) and 1064 nm (b). The thickness of nanowires is 4 nm. (c) The smaller value of the two absorption efficiencies.

conventional SNSPDs with Ag slots are lower than 50% for both wavelengths. It is a significant improvement to the conventional SNSPDs in terms of the filling factor. Then the relationship between the absorption efficiency and the cavity length was investigated, as shown in Fig. 2(b). The pitch lengths were fixed to the optimum values. The absorption efficiencies of the proposed SNSPD increase to the maximum for two wavelengths when the cavity length is about 400 nm. In addition, the absorption efficiency for the 1064 nm wave is more sensitive than that for the 1550 nm wave as the cavity length changed. This demonstrates the cavity effect in the structure for both wavelengths.[13] However, the absorption efficiency of conventional SNSPDs with Ag slots is poor when the pitch is large. When the structure parameters and the incident light wavelength are changed, the distribution of the electric field is also changed because Si, a high-index dielectric, was applied as the slot material. It compensates the dielectric mismatch between the NbN nanowire and the cavity material and has a strong transmission of light at the wavelength of 1550 nm and 1064 nm compared to Ag. When the value of the structure parameter reaches a special range, the absorption efficiency has an increment because the electric field intensity in the region of the nanowires is greatly enhanced. In order to see this performance more intuitively, we investigated the distribution of the electric field in the period unit of the optimum pitch for the two different wavelengths, as shown in Fig. 3. The electric field intensity in the Si–HSQ–Si slots, especially in the region where the NbN nanowires are placed is higher than that in other areas. In addition, the distributions have the same phenomenon for the two target wavelengths. As obtained from Eq. (1), the high electric field intensity within the nanowires corresponds to the high absorption efficiency. It demonstrates that the absorption efficiency can also be high under the condition of low-filling-factor nanowires due to the proposed structure.

The pitch and the cavity length are considered independent in the analysis above, which directly demonstrates that a high absorption efficiency can be obtained when the pitch and cavity length are in the special value ranges. However, we are more concerned about the robustness to fabrication uncertainties than those specific optimum values. Moreover, to investigate the correlations between
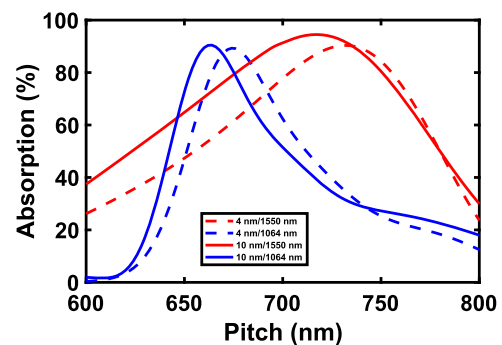

FIG. 5. Simulated pitch dependence of the optical absorption efficiency for different incident light wavelengths and thicknesses of the nanowires.
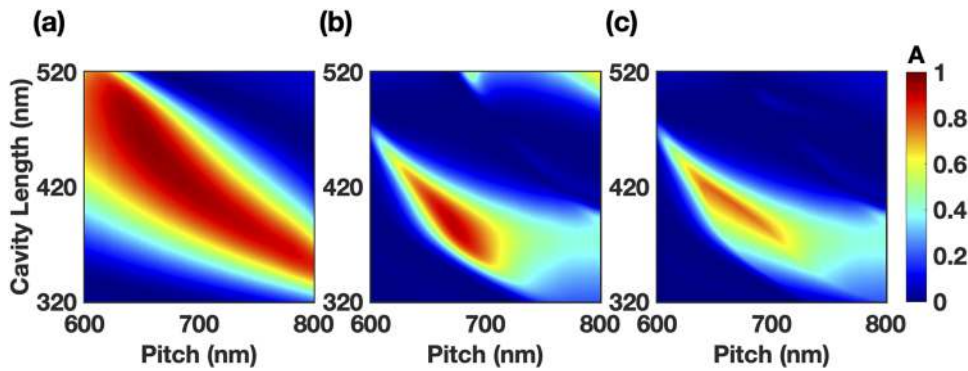
FIG. 6. Simulated structure parameters dependence of the optical absorption efficiency. The incident light wavelengths are 1550 nm (a) and 1064 nm (b). The thickness of nanowires is 10 nm. (c) The smaller value of the two absorption efficiencies.

these structure parameters and the absorption efficiency comprehensively, both the pitch and the cavity length were considered simultaneously. The correlations between the two structure parameters and the absorption efficiency for two wavelengths are shown in Fig. 4. It is obvious that the absorption efficiency can be over 80%, even 90%, in a parameter range, for each wavelength. In addition, the satisfied parameter range of 1550 nm is larger than that of 1064 nm. This is consistent with the results in Fig. 2. The smaller value of these two absorption efficiencies of two wavelengths is also illustrated in Fig. 4(c). This indicates the minimum absorption efficiency the SNSPD can achieve when it works with two wavelengths at the same time. From Fig. 4(c), a narrow parameter range can be obtained, which satisfies the condition of the absorption efficiency exceeding 80% for both work wavelengths. Meanwhile, the filling-factors of nanowires are all very low due to the large pitches in the parameter area. So the multispectral SNSPDs with high absorption efficiency and low-filling-factor (about 12%) nanowires can be obtained by using the satisfied structure parameters in Fig. 4(c).

Considering the errors in realistic fabrication, the narrow optimal parameter range is better to be expanded. We increased the thickness of nanowires to enhance the ability of absorbing photons.[18] So the thickness of the nanowires is increased to 10 nm. The calculated absorption efficiency dependence of the pitch for different wavelengths is indicated in Fig. 5. For comparison, the results of the 4 nm nanowires are also shown. The optical absorption efficiency of the nanowires is also over 90% for each wavelength, though the pitch is about 718 nm or 664 nm. The intersection of two solid curves indicates that the absorption efficiency can be about 80% for both wavelengths when the pitch is about 676 nm. The intersection of solid curves is on the top left of the intersection of dashed curves, which demonstrates that the absorption efficiency of the 10 nm nanowires is higher than that of the 4 nm nanowires, though the pitch is slightly smaller, and then, the correlations between the two structure parameters and absorption efficiency for two wavelengths are shown in Fig. 6. It is obvious that the satisfied parameter range in Fig. 6(c) is larger than that in Fig. 4(c). It means that the tolerance for the fabrication errors is enhanced. So the satisfied parameter range is expanded and the absorption efficiency is further improved due to the thicker nanowires. It should be noted that the nanowires with the thickness over 10 nm are hardly selected in realistic fabrication because for these thicknesses of nanowires, they are hard to achieve saturation of the internal detection.[23,24]

III. COUNTING RATE

Another important parameter is the counting rate, which describes the detection speed of SNSPDs. The overall non-sensitive time of the SNSPD consists of two parts. One is the rise time of the voltage pulse, which is determined by the time-dependent hotspot resistance and the load impedance. The other is the decay time of the voltage pulse, which is determined by the kinetic inductance of the nanowire. Because the decay time is much longer than the rise time, the reset time can be reduced considerably by reducing the kinetic inductance.[11] The kinetic inductance of the nanowire is defined as[25]

$$L_k = \mu_0 \lambda^2 l / S, \qquad (2)$$

where μ_0 is the vacuum permeability, λ is the penetration depth, l is the nanowire length, and S is the cross-section area of the nanowire. The reset time (denoted by τ) is defined as the time needed for the device efficiency recovering up to 90% of the device efficiency in the origin state after a detection event. Thereby, the reset time is also defined as the time needed for the current to recover from 0 to $I_{90\%}$ by[13]

$$\tau = \frac{L_k}{R} \ln\left[1 / \left(1 - \frac{I_{90\%}}{I_b} \right) \right], \qquad (3)$$

where I_b is the bias current, $I_{90\%}$ is the current when the device efficiency is 90% of the device efficiency at I_b, and $R = 50 \ \Omega$. Generally, we assumed that $I_b = 0.95 I_c$, where I_c is the critical current of superconducting nanowires, and $I_{90\%} = 0.9 I_c$. After the simulations and calculations, the filling-factor of our proposed SNSPD is about 12%; however, the filling-factor of the conventional SNSPDs is about 50%. It is assumed that these two kinds of devices have active areas of the same size and nanowires of the same cross-sectional area. The length of 12%-filling-factor nanowires is about 24% of the length of 50%-filling-factor nanowires, and the result is the same as L_k, which can be obtained from Eq. (2). So it can be roughly estimated from Eq. (3) that the reset time of our proposed SNSPD is about 24% of the conventional SNSPDs. This indicates that our proposed SNSPD has a better performance in the high-speed detection situations.

IV. CONCLUSION

In conclusion, we have proposed a multispectral and low-filling-factor SNSPD, which can achieve a high absorption efficiency and a high counting rate at two target wavelengths simultaneously. Due to the Si–HSQ–Si slots and the Ag reflector, a high absorption efficiency can be achieved even for the low-filling-factor

nanowires whether the incident light wavelength is 1550 nm or 1064 nm. In addition, the satisfied structure parameter range is also shown. Meanwhile, to reduce the fabrication difficulty and to further improve the absorption efficiency, the optimal parameter range is expanded by using the thicker nanowires. The reset time of our proposed SNSPDs is about 24% of the conventional SNSPDs, so it will have a better performance in high-speed detection situations. The designed SNSPD in this paper provides access to fabricate multispectral SNSPDs with a high absorption efficiency and a high counting rate, which can be applied in many optics applications, such as quantum optics communication and multiwavelength sensing.

ACKNOWLEDGMENTS

DATA AVAILABILITY

The data that support the findings of this study are available within the article.

REFERENCES

[1]G. N. Gol'tsman, O. Okunev, G. Chulkova, A. Lipatov, A. Semenov, K. Smirnov, B. Voronov, A. Dzardanov, C. Williams, and R. Sobolewski, Appl. Phys. Lett. **79**, 705–707 (2001).

[2]F. Marsili, V. B. Verma, J. A. Stern, S. Harrington, A. E. Lita, T. Gerrits, I. Vayshenker, B. Baek, M. D. Shaw, R. P. Mirin, and S. W. Nam, Nat. Photonics **7**, 210–214 (2013).

[3]E. E. Wollman, V. B. Verma, A. D. Beyer, R. M. Briggs, B. Korzh, J. P. Allmaras, F. Marsili, A. E. Lita, R. P. Mirin, S. W. Nam, and M. D. Shaw, Opt. Express **25**, 26792–26801 (2017).

[4]J. Huang, W. Zhang, L. You, C. Zhang, C. Lv, Y. Wang, X. Liu, H. Li, and Z. Wang, Supercond. Sci. Technol. **31**, 074001 (2018).

[5]I. Esmaeil Zadeh, J. W. N. Los, R. B. M. Gourgues, V. Steinmetz, G. Bulgarini, S. M. Dobrovolskiy, V. Zwiller, and S. N. Dorenbos, APL Photonics **2**, 111301 (2017).

[6]N. Calandri, Q.-Y. Zhao, D. Zhu, A. Dane, and K. K. Berggren, Appl. Phys. Lett. **109**, 152601 (2016).

[7]H.-L. Yin, T.-Y. Chen, Z.-W. Yu, H. Liu, L.-X. You, Y.-H. Zhou, S.-J. Chen, Y. Mao, M.-Q. Huang, W.-J. Zhang, H. Chen, M. J. Li, D. Nolan, F. Zhou, X. Jiang, Z. Wang, Q. Zhang, X.-B. Wang, and J.-W. Pan, Phys. Rev. Lett. **117**, 190501 (2016).

[8]Y. Liu, Q. Zhao, M.-H. Li, J.-Y. Guan, Y. Zhang, B. Bai, W. Zhang, W.-Z. Liu, C. Wu, X. Yuan, H. Li, W. J. Munro, Z. Wang, L. You, J. Zhang, X. Ma, J. Fan, Q. Zhang, and J.-W. Pan, Nature **562**, 548–551 (2018).

[9]L. Xue, Z. Li, L. Zhang, D. Zhai, Y. Li, S. Zhang, M. Li, L. Kang, J. Chen, P. Wu, and Y. Xiong, Opt. Lett. **41**, 3848–3851 (2016).

[10]Q.-Y. Zhao, D. Zhu, N. Calandri, A. E. Dane, A. N. McCaughan, F. Bellei, H.-Z. Wang, D. F. Santavicca, and K. K. Berggren, Nat. Photonics **11**, 247–251 (2017).

[11]C. M. Natarajan, M. G. Tanner, and R. H. Hadfield, Supercond. Sci. Technol. **25**, 063001 (2012).

[12]K. M. Rosfjord, J. K. W. Yang, E. A. Dauler, A. J. Kerman, V. Anant, B. M. Voronov, G. N. Gol'tsman, and K. K. Berggren, Opt. Express **14**, 527–534 (2006).

[13]X. Hu, E. A. Dauler, R. J. Molnar, and K. K. Berggren, Opt. Express **19**, 17–31 (2011).

[14]S. Ferrari, C. Schuck, and W. Pernice, Nanophotonics **7**, 1725–1758 (2018).

[15]V. B. Verma, B. Korzh, F. Bussières, R. D. Horansky, A. E. Lita, F. Marsili, M. D. Shaw, H. Zbinden, R. P. Mirin, and S. W. Nam, Appl. Phys. Lett. **105**, 122601 (2014).

[16]L. Redaelli, G. Bulgarini, S. Dobrovolskiy, S. N. Dorenbos, V. Zwiller, E. Monroy, and J. M. Gérard, Supercond. Sci. Technol. **29**, 065016 (2016).

[17]H. Li, H. Wang, L. You, P. Hu, W. Shen, W. Zhang, X. Yang, L. Zhang, H. Zhou, Z. Wang, and X. Xie, Opt. Express **27**, 4727–4733 (2019).

[18]T. Yamashita, S. Miki, H. Terai, and Z. Wang, Opt. Express **21**, 27177–27184 (2013).

[19]A. Engel, J. J. Renema, K. Il'in, and A. Semenov, Supercond. Sci. Technol. **28**, 114003 (2015).

[20]A. J. Kerman, E. A. Dauler, W. E. Keicher, J. K. W. Yang, K. K. Berggren, G. Gol'tsman, and B. Voronov, Appl. Phys. Lett. **88**, 111116 (2006).

[21]V. Anant, A. J. Kerman, E. A. Dauler, J. K. W. Yang, K. M. Rosfjord, and K. K. Berggren, Opt. Express **16**, 10750–10761 (2008).

[22]S. Miki, T. Yamashita, H. Terai, and Z. Wang, Opt. Express **21**, 10208–10214 (2013).

[23]W. Zhang, Q. Jia, L. You, X. Ou, H. Huang, L. Zhang, H. Li, Z. Wang, and X. Xie, Phys. Rev. Appl. **12**, 044040 (2019).

[24]K. Smirnov, A. Divochiy, Y. Vakhtomin, P. Morozov, P. Zolotov, A. Antipov, and V. Seleznev, Supercond. Sci. Technol. **31**, 035011 (2018).

[25]X. Tao, S. Chen, Y. Chen, L. Wang, X. Li, X. Tu, X. Jia, Q. Zhao, L. Zhang, L. Kang, and P. Wu, Supercond. Sci. Technol. **32**, 064002 (2019).